

The TauP Toolkit: Flexible Seismic Travel-Time and Raypath Utilities

H. Philip Crotwell, Thomas J. Owens, Jeroen Ritsema
Department of Geological Sciences University of South Carolina

For Submittal: Seismological Research Letters, Jan. 1999

Introduction

The calculation of travel times and ray paths of seismic phases for a specified velocity model of the earth has always been a fundamental need of seismologists. In recent years, the number of different phases used in analysis has been growing as has the availability of new earth models, especially models developed from detailed regional studies. These factors highlight the need for versatile utilities that allow the calculation of travel times and raypaths of (ideally) any conceivable seismic phase passing through (ideally) arbitrary velocity models. The method of Buland and Chapman (1983) provides significant progress toward this need by allowing for the computation of times and paths of any rays passing through arbitrary spherically-symmetric velocity models. The implementation of this method through the *ttimes* software program (Kennett and Engdahl, 1991) for a limited number of velocity models and a standard set of seismic phases has been widely used in the seismological community. In this paper, we describe a new implementation of the method of Buland and Chapman (1983) that easily allows for the use of arbitrary spherically-symmetric velocity models and arbitrary phases. This package, the TauP Toolkit, provides for the computation of phase travel-times, travel-time curves, raypaths through the earth, and phase piercing-points in a publicly-available, machine-independent package that should be of use both to practicing seismologists and in teaching environments.

Methodology

The method of Buland and Chapman (1983) works in the delay (or intercept) time (τ) - ray parameter (p) domain to avoid complications of multi-valued travel-time branches associated with working in the time-distance domain directly. Physically, τ is the zero-distance intercept and p is the slope of the line tangent to the travel-time curve at a given distance. The advantages of working in this domain are that τ -branches are monotonic and single valued in all cases, and thus they do not suffer from the problems of triplications as their corresponding travel-time branches may in some circumstances. Furthermore, the ray parameters that define each τ branch are simple and well-defined functions of the earth model. We will not describe the method in any detail, but we will discuss the general steps necessary to implement this approach. We used Maple (Heal et al., 1996), a symbolic mathematics utility, to help convert the equations in Buland and Chapman (1983) to algorithmic forms for a spherical coordinate system, avoiding the additional complication of an earth flattening transform. The resulting Maple files are provided with the TauP Toolkit distribution for those interested in a more detailed study of the methodology.

Generating travel-times using the method of Buland and Chapman (1983) consists of four major steps. The first is sampling the velocity-depth model in slowness. Next is integrating the slowness to get distance and time increments for individual model branches. A "branch" of a model is a depth range bounded above and below by local slowness extrema (first-order discontinuities or reversals in slowness gradients). A sum of these model branches along a particular path results in the corresponding branch of the travel time curves. These first two steps are undertaken in the *taup_create* utility and need only be done once for each new velocity model. The third step involves summing the branches along the path of a specified phase. Finally, an interpolation between time-distance

samples is required to obtain the time of the exact distance of interest. These final steps are undertaken in various TauP Toolkit utilities, depending on the information that is desired by the user.

Slowness Sampling

Creating a sufficiently dense sampling in slowness from the velocity models is the most complicated and crucial step. There are several qualifications for a sufficiently dense sampling. First, all critical points must be sampled exactly. These include each side of first-order discontinuities and all reversals in slowness gradient. Less obvious points that must be sampled exactly occur at the bottom of a low velocity zone. This sample is the turning point for the first ray to turn below the zone. Note, it is possible for the velocity to decrease with depth but, due to the curvature of the earth, there may not be any of the pathological effects. For example, PREM (Dziewonski and Anderson, 1981) contains a low velocity layer below the moho, but rays turn throughout it. Hence, a more strictly accurate term might be “high slowness zones”.

A second sampling condition is that slowness samples must be sufficiently closely spaced in depth. This is normally satisfied by the depth sampling interval of the velocity model itself, but additional samples may need to be inserted. A third condition is that the sampling interval must be sufficiently small in slowness. We satisfy this condition by inserting slowness samples whenever the increment in slowness is larger than a given tolerance simultaneously solving for the corresponding depth using the original velocity model.

Finally, the resulting slowness sampling must not be too coarse in distance, as measured by the resulting distance sampling for the direct P or S wave from a surface source. Our approach to satisfying this condition is similar to that of the previous condition. We insert new slowness samples whenever the difference in total distance between adjacent direct rays from a surface source exceeds the given tolerance. Again, the depth corresponding to the inserted slowness sample is computed from the original velocity model. As an additional precaution against undersampling, we also check to make sure that the curvature is not too great for linear interpolation to be reasonable. This is accomplished by comparing the time at each sample point with the value predicted from linear interpolation from the previous to the next point. If this exceeds a given tolerance, then additional samples are inserted before and after the point. The last two conditions require the most computational effort but also have the most effect in creating a sufficiently well-sampled model. The sampling for P and S must meet these conditions individually and, in order to allow for phase conversions, must be compatible with each other.

Branch Integration, Phase Summing and Interpolation

For each region, or branch, of the model, we merely sum the distance and time contributions from each slowness layer, between slowness samples, for each ray parameter. Within each layer we use the Bullen law $v(r) = Ar^B$, which has an analytic solution. The ray parameters used are the subset of slowness samples that correspond to turning or critically reflected rays from a surface source. Care must be taken to avoid summing below the turning point for each slowness.

Once these “branches” have been constructed, it is straightforward to create a real branch of the travel time curves by an appropriate summing. Of course, the maximum and minimum allowed ray parameter must be determined in order to assure that the ray can actually propagate throughout these regions. For instance, the branch summing for a P wave turning in the mantle and for PcP are the same. However, the ray parameter for any P phase must be larger than the slowness at the bottom of the mantle, while that for PcP must be smaller.

Once the sum has been completed to create time, distance and tau as a function of ray parameter, an interpolation between known points must be done to calculate arrivals at intermediate distances. Currently, we use a simple linear interpolation which is sufficient for most purposes. More advanced interpolations do provide advantages in reducing the number of samples needed to achieve a given accuracy, but they can have certain instability or oscillatory problems that are difficult to deal with when the model is not known in advance.

Figure 1 summarizes the effect of two choices of sampling parameters using the IASP91 model (Kennett and Engdahl, 1991). In Figure 1a, we illustrate that our normal sampling (model file: *iasp91*) produces a relatively small residual, maximum of 0.013 seconds for P and 0.016 seconds for S, relative to a highly oversampled version of the same model generated to produce the most accurate time estimates without regard to model size or computation time. Thus, model *iasp91* is likely the appropriate choice for travel times that will be used in further computations, for instance in earthquake location studies. However, the model size is 337Kb, which may be slow to load on some computer systems and does increase the computation time somewhat. A more coarsely sampled version of IASP91, which we distribute in model file *qdt* (*quick and dirty times*), sacrifices some accuracy for a smaller model file. Figure 1b shows *qdt* residuals with respect to the same highly oversampled model. There are larger and more noticeable peaks due to linear interpolation between the more widely spaced samples. While this would not make a good choice for earthquake location work, an error of 0.25 seconds is entirely satisfactory for classroom work, for determining windows for extracting phases, and for getting quick estimates of arrival times. Most important is the fact that the decision of how accurately the model needs to be sampled is left up to the user. One can easily create new samplings of existing models tailored to the requirements of the job at hand.

Figure 2 compares TauP results using IASP91 to output from *ttimes*. It would be desirable to compare the *ttimes* output with our own for a model with an easy analytic solution over a range of distances and phases. Unfortunately, using different models with the *ttimes* program has proven difficult. The residual for the direct comparison with *ttimes* is shown for the first arriving P wave and S wave. The calculations are for the IASP91 model for an event at the surface and are sampled at 0.1 degree increments. The high frequency variations in residuals, such as are observed between 50 and 90 degrees in the P-wave residuals, are the result of the use of the linear interpolation in TauP. We believe that the clear trend of increasingly negative relative residuals with increasing distance is likely related to the use of an earth flattening transform within the *ttimes* package, an approximation that can become problematical toward the center of the earth. The TauP package avoids this potential complication by working directly in spherical coordinates. To test this assertion, we compared *ttimes* and TauP results to travel-times calculated by numerical integration of vertical rays of PcP, PKIKP, and PKiKP through the IASP91 model. In each case, our results were closer to the numerical integration results than *ttimes*, with the *ttimes* error increasing with increasing depth of penetration. The maximum difference of 0.01 sec for TauP compared to 0.05 sec for *ttimes* for the vertical PKIKP ray accounts for the relative P residual shown in Figure 2. Thus, we expect that our solutions have a small, but possibly significant, increase in accuracy relative to *ttimes*, in spite of the current simple linear interpolation.

Seismic Phase Name Parsing

A major feature of the TauP Toolkit is the implementation of a phase name parser that allows the user to define essentially arbitrary phases through the earth. Thus, the TauP Toolkit is extremely flexible in this respect since it is not limited to a pre-defined set of phases. Phase names are not hard-coded into the software, but rather the names are interpreted and the appropriate propagation path and resulting times are constructed at run time. Designing a phase-naming convention that is general enough to support arbitrary phases and easy to understand is an essential and somewhat challenging step. The rules that we have developed are described here. Most of phases resulting from these conventions should be familiar to seismologists, e.g. pP, PP, PcS, PKiKP, etc. However, the uniqueness required for parsing results in some new names for other familiar phases.

In traditional “whole-earth” seismology, there are 3 major interfaces: the free surface, the core-mantle boundary, and the inner-outer core boundary. Phases interacting with the core-mantle boundary and the inner core boundary are easy to describe because the symbol for the wave type changes at the boundary (i.e., the symbol P changes to K within the outer core even though the wave type is the same). Phase multiples for these interfaces and the free surface are also easy to describe because the symbols describe a unique path. The challenge begins with the description of interactions with interfaces within the crust and upper mantle. We have introduced two new symbols to existing nomenclature to provide unique descriptions of potential paths. Phase names are constructed from a sequence of symbols and numbers (with no spaces) that either describe the wave type, the interaction a

wave makes with an interface, or the depth to an interface involved in an interaction. Figure 3 shows examples of interactions with the 410km discontinuity using our nomenclature.

1. Symbols that describe wave-type are:

- P compressional wave, upgoing or downgoing, in the crust or mantle
- p strictly upgoing P wave in the crust or mantle
- S shear wave, upgoing or downgoing, in the crust or mantle
- s strictly upgoing S wave in the crust or mantle
- K compressional wave in the outer core
- I compressional wave in the inner core
- J shear wave in the inner core

2. Symbols that describe interactions with interfaces are:

- m interaction with the moho
- g appended to P or S to represent a ray turning in the crust
- n appended to P or S to represent a head wave along the moho
- c topside reflection off the core mantle boundary
- i topside reflection off the inner core outer core boundary
- ^ underside reflection, used primarily for crustal and mantle interfaces
- v topside reflection, used primarily for crustal and mantle interfaces
- diff appended to P or S to represent a diffracted wave along the core mantle boundary
- kmps appended to a velocity to represent a horizontal phase velocity (see 10 below)

3. The characters **p** and **s** **always** represent up-going legs. An example is the source-to-surface leg of the phase **pP** from a source at depth. **P** and **S** can be turning waves but always indicate downgoing waves leaving the source when they are the first symbol in a phase name. Thus, to get near-source, direct P-wave arrival times, you need to specify two phases, **p** and **P**, or use the “*times* compatibility phases” described below. However, **P** may represent an upgoing leg in certain cases. For instance, **PcP** is allowed since the direction of the phase is unambiguously determined by the symbol **c**, but it would be named **PcP** by a purist using our nomenclature.
4. Numbers, except velocities for **kmps** phases (see 10 below), represent depths at which interactions take place. For example, **P410s** represents a P-to-S conversion at a discontinuity at 410 km depth. Since the S-leg is given by a lower-case symbol and no reflection indicator is included, this represents a P-wave converting to an S-wave when it hits the interface from below. The numbers given need not be the actual depth; instead the closest depth corresponding to a discontinuity in the model will be used. For example, if the time for **P410s** is requested in a model where the discontinuity was really located at 406.7 kilometers depth, the time returned would actually be for **P406.7s**. The code “*taup time*” would note that this had been done. Obviously, care should be taken to ensure that there are no other discontinuities closer than the one of interest, but this approach allows generic interface names like “410” and “660” to be used without knowing the exact depth in a given model.
5. If a number appears between two phase legs, e.g. **S410P**, it represents a transmitted phase conversion, not a reflection. Thus, **S410P** would be a transmitted conversion from S to P at 410 km depth. Whether the conversion occurs on the down-going side or up-going side is determined by the upper or lower case of the following leg. For instance, the phase **S410P** propagates down as an S, converts at the 410 to a P, continues down, turns as a P wave, and propagates back across the 410 and to the surface. **S410p** on the other hand, propagates down as an S through the 410, turns as an S, hits the 410 from the bottom, converts to a **p** and then goes up to the surface. In these examples, the case of the phase symbol (P vs. p) is critical because the direction of propagation (upgoing or downgoing) is not unambiguously defined elsewhere in the phase name. The importance is clear when you consider a source depth below 410 compared to above 410. For a source depth greater than 410 km, **S410P** technically cannot exist while **S410p** maintains the same path (a receiver side conversion) as it does for a source depth above the 410.

The first letter can be lower case to indicate a conversion from an up-going ray, e.g. $p410S$ is a depth phase from a source at greater than 410 km depth that phase converts at the 410 discontinuity. It is strictly upgoing over its entire path and hence could also be labeled $p410s$. $p410S$ is often used to mean a reflection in the literature, but there are too many possible interactions for the phase parser to allow this. If the underside reflection is desired, use the $\hat{p}410S$ notation from rule 7.

6. Due to the two previous rules, $P410P$ and $S410S$ are over-specified but still legal. They are almost equivalent to P and S , respectively, but restrict the path to phases transmitted through (turning below) the 410. This notation is useful to limit arrivals to just those that turn deeper than a discontinuity (thus avoiding travel-time curve triplications), even though they have no real interaction with it.
7. The characters $\hat{}$ and \vee are new symbols introduced here to represent bottom-side and top-side reflections, respectively. They are followed by a number to represent the approximate depth of the reflection or a letter for standard discontinuities, m , c or i . Reflections from discontinuities besides the core-mantle boundary c or inner-core outer-core boundary i must use the $\hat{}$ and \vee notation. For instance, in the TauP convention, $\hat{p}410S$ is used to describe a near-source underside reflection.

Underside reflections, except at the surface (PP , sS , etc.), core-mantle boundary ($PKKP$, $SKKS$, etc.), or outer-core-inner-core boundary ($PKIKP$, $SKJKS$, $SKIKS$, etc.), must be specified with the $\hat{}$ notation. For example, $\hat{P}410P$ and $\hat{P}mP$ would both be underside reflections from the 410 km discontinuity and the Moho, respectively.

The phase PmP , the traditional name for a top-side reflection from the Moho discontinuity, must change names under our new convention. The new name is $PvmP$ or $Pvmp$ while PmP just describes a P wave that turns beneath the Moho. The reason the Moho must be handled differently from the core-mantle boundary is that traditional nomenclature did not introduce a phase change symbol at the Moho. Thus, while PcP makes sense since a P -wave in the core would be labeled K , PmP could have several meanings. The m symbol just allows the user to describe phases interaction with the Moho without knowing its exact depth. In all other respects, the $\hat{}$ - \vee nomenclature is maintained.

8. Currently, $\hat{}$ and \vee for non-standard discontinuities are allowed only in the crust and mantle. Thus, there are no reflections off non-standard discontinuities within the core (reflections such as $PKKP$, $PKiKP$ and $PKIKP$ are still fine). There is no reason in principle to restrict reflections off discontinuities in the core, but until there is interest expressed, these phases will not be added. Also, a naming convention would have to be created since “ p is to P ” is not the same as “ i is to I ”.
9. Currently there is no support for $PKPab$, $PKPbc$, or $PKPdf$ phase names. They lead to increased algorithmic complexity that at this point seems unwarranted. Currently, in regions where triplications develop, the triplicated phase will have multiple arrivals at a given distance. So, $PKPab$ and $PKPbc$ are both labeled just PKP while $PKPdf$ is called $PKIKP$.
10. The symbol $kmps$ is used to get the travel time for a specific horizontal phase velocity. For example, $2kmps$ represents a horizontal phase velocity of 2 km/sec. While the calculations for these are trivial, it is convenient to have them available to estimate surface-wave travel times or to define windows of interest for given paths.
11. As a convenience, a *times* phase name compatibility mode is available. So ttp gives you the phase list corresponding to P in *times*. Similarly there are tts , $ttp+$, $tts+$, $ttbasic$ and $ttall$.

Velocity Model Descriptions

This version of the TauP package supports two types of velocity model files. Both are piecewise linear between given depth points. Support of cubic spline velocity models would be useful and may be implemented in a future release.

The first format is the “tvel” format used by the most recent *ttimes* code (Kennett et al., 1995). This format has two comment lines, followed by lines composed of depth, Vp, Vs, and density, all separated by whitespace. TauP ignores the first two lines and reads the remaining ones.

The second format is based on the format used by Xgbm (Davis and Henson, 1993). We refer to it as a “named discontinuity” format. Its biggest advantage is that it can specify the location of major boundaries in the earth. It is our preferred format. The format also provides density and attenuation fields, which will more easily accommodate the calculation of synthetic seismograms in the future.

The distribution comes with several standard velocity models. Users can create their own models by following examples in the *User's Guide* included in the distribution package. Standard models are: IASP91 (Kennett and Engdahl, 1991), PREM (Dziewonski and Anderson, 1981), AK135 (Kennett et al., 1995), Jeffries-Bullen (Jeffreys and Bullen, 1940), 1066a and 1066b (Gilbert and Dziewonski, 1975), PWDK (Weber and Davis, 1990), SP6 (Morelli and Dziewonski, 1993), and Herrin (Herrin, 1968).

Utilities in the TauP Toolkit

There are 8 separate utilities in the TauP Toolkit. Each is described in detail in the *User's Guide*, so descriptions here are brief. Figure 4 summarizes the outputs of several of the codes.

1. `taup_create`. This utility takes a velocity model in one of the two supported formats and does the sampling and branch integration processes to produce a TauP model file for use by all other utilities.
2. `taup_time`. This is the TauP replacement for the *ttimes* program. At a minimum, given phase, distance and depth information, it returns travel times and ray parameters. Options allow for station and event locations to be provided in lieu of distance as well as for more specialized outputs.
3. `taup_curve`. Produces entire travel time curves for given phases. Options include the ability to output these curves in a format suitable for plotting with GMT (Wessel and Smith, 1995).
4. `taup_path`. Calculates ray paths for given phases. Options include the ability to output these paths in a format suitable for plotting with GMT (Wessel and Smith, 1995).
5. `taup_pierce`. Calculates piercing points at model discontinuities and at specified depths for given phases. Options include the ability to output these points in a format suitable for plotting with GMT (Wessel and Smith, 1995).
6. `taup_setsac`. Utility to fill SAC (Tull, 1989) file headers with theoretical arrival times.
7. `taup_table`. Utility to generate travel-time tables needed for earthquake location programs. Currently, only an ASCII table format is supported along with a generic output. Other formats could be supported if interest warrants.
8. `taup_peek`. Debugging code to examine contents of a taup velocity model file.

The TauP Toolkit is written entirely in the Java programming language. This should facilitate use of the utilities on any major computer platform. It has been tested on Solaris UNIX, MacOS, and Windows95. The distribution includes simple scripts to facilitate use of the above utilities in a UNIX environment. It also provides mechanisms for accessing the utilities via C programs and TCL (via the “jacl” implementation) scripts. At present, only raw Java command line interfaces exist, limiting the usefulness in MacOS and Windows environments. A WWW based applet interface was tested by our undergraduate geophysics course in the spring of 1998, but a more refined GUI is planned for development soon which should make the package much more useful in non-UNIX environments. The package can be obtained from <http://www.seis.sc.edu>.

Acknowledgments

Development of this software was supported by the University of South Carolina. Manuscript preparation and software testing were supported by NSF grant EAR-9304657.

References

- Buland, R. and C. H. Chapman (1983). The computation of seismic travel times, *Bull. Seism. Soc. Am.* **73**, 1271–1302.
- Davis, J. P. and I. H. Henson (1993). *User's Guide to Xgbm: An X-Windows System to compute Gaussian beam synthetic seismograms* (1.1 ed.), Alexandria, VA: Teledyne Geotech Alexandria Laboratories.
- Dziewonski, A. M. and D. L. Anderson (1981). Preliminary reference earth model, *Phys. Earth Planet. Interiors* **25**, 297–356.
- Gilbert, F. and A. M. Dziewonski (1975). An application of normal mode theory to the retrieval of structural parameters and source mechanisms from seismic spectra, *Phil. Trans. Roy. Soc., Lond. A* **278**, 187–269.
- Heal, K. M., M. L. Hansen, and K. M. Rickard (1996). *Maple V Learning Guide*, Springer-Verlag.
- Herrin, E. (1968). 1968 seismological tables for P phases, *Bull. Seism. Soc. Am.* **58**, 1193–1241.
- Jeffreys, H. and K. E. Bullen (1940). *Seismological Tables*, London: British Association for the Advancement of Science, Burlington House.
- Kennett, B. L. N. and E. R. Engdahl (1991). Traveltimes for global earthquake location and phase identification, *Geophys. J. Int.* **105**, 429–465.
- Kennett, B. L. N., E. R. Engdahl, and R. Buland (1995). Constraints on seismic velocities in the Earth from traveltimes, *Geophys. J. Int.* **122**, 108–124.
- Morelli, A. and A. M. Dziewonski (1993). Body wave traveltimes and a spherically symmetric P- and S-wave velocity model, *Geophys. J. Int.* **112**, 178–194.
- Tull, J. E. (1989). *SAC - Seismic Analysis Code: User's Manual* (Rev. 2), Livermore, CA: Lawrence Livermore National Laboratory.
- Weber, M. and J. P. Davis (1990). Evidence of a laterally variable lower mantle structure from P- and S-waves, *Geophys. J. Int.* **102**, 231–255.
- Wessel, P. and W. H. F. Smith (1995). New Version of the Generic Mapping Tools released, *Eos Trans. Am. Geophys. U.* **76**, 329.

Figure Captions

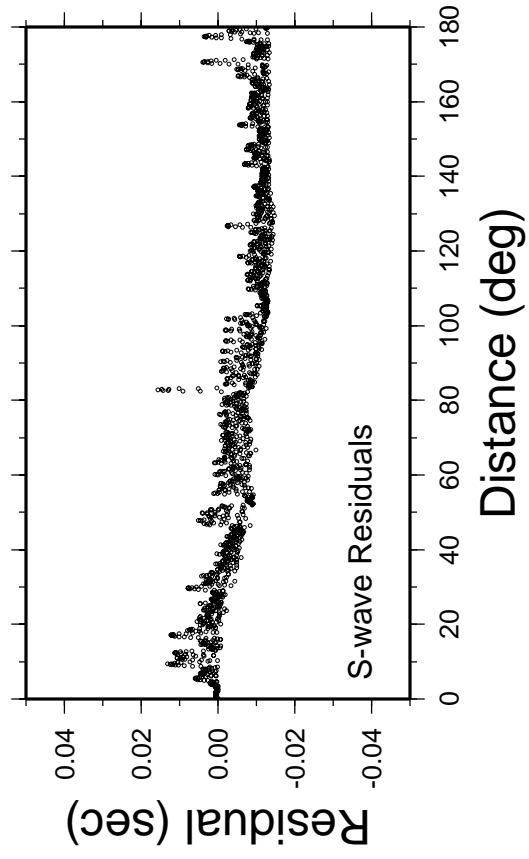
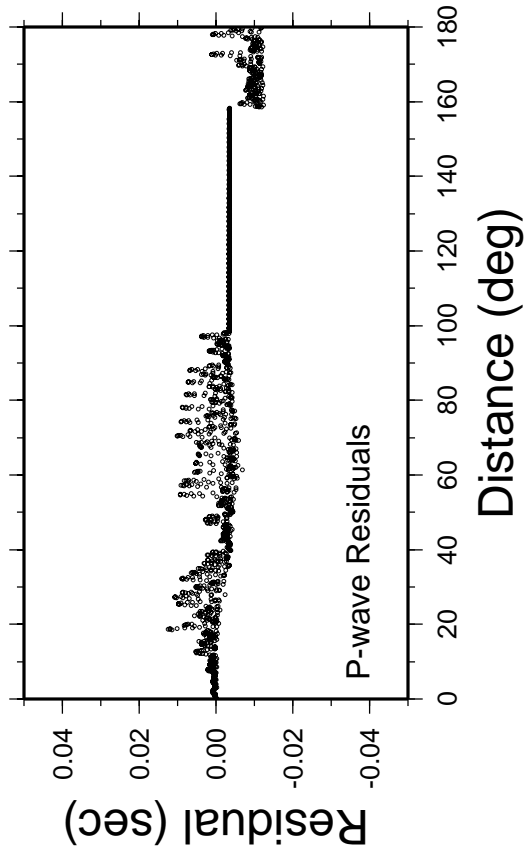
Figure 1a. First arriving P (top) and S (bottom) residual between a highly oversampled IASP91 model and the default sampling. The time residual is sampled every tenth of a degree and is within 0.013 seconds for P and 0.016 seconds for S over the entire distance range. The slight trend to increasingly negative residuals with distance is the result of using a less dense linear interpolation of the original cubic IASP91 velocity model. While the difference associated with this trend is small, about 0.01 seconds at 180 degrees, adding the ability to read cubic splines directly should eliminate it.

Figure 1b. First arriving P (top) and S (bottom) residual between a highly oversampled IASP91 model and a coarsely sampled model. This less well sampled version of IASP91 is referred to as *qdt* and is shown to illustrate the flexibility of the model sampling process. It has much larger errors, about ± 0.25 seconds, but is one quarter the size (83Kb) and is therefore more suitable for quick travel-time estimates, classroom exercises and web based applications where size and loading speed are more critical than accuracy. Note the factor of 10 change in scale from the previous figure.

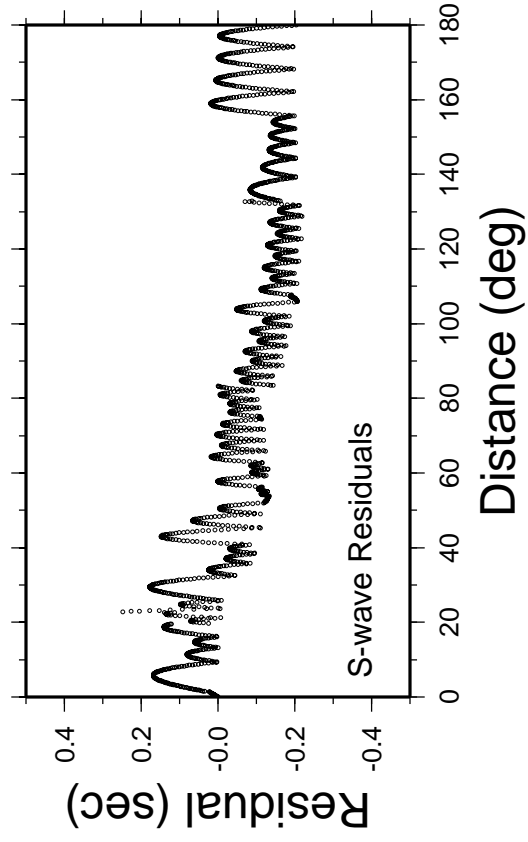
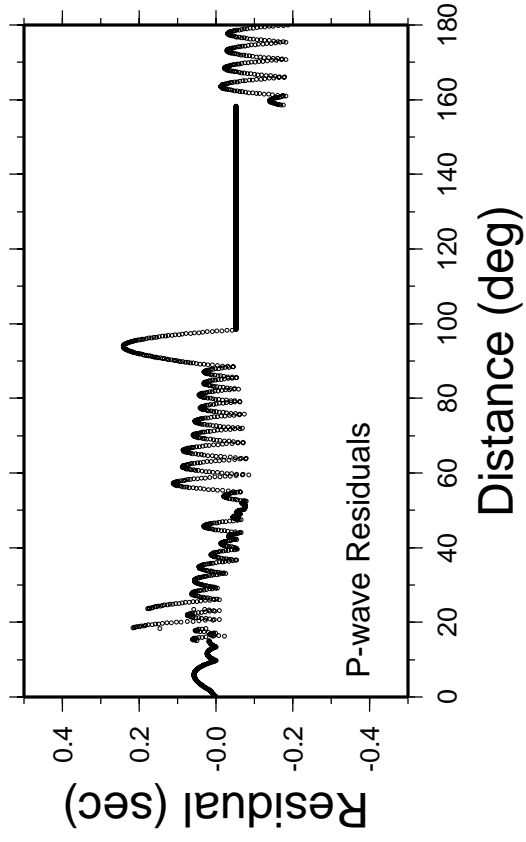
Figure 2. Residual travel time, this code minus *ttimes*, of the first arriving P wave (top) and first arriving S wave (bottom). The compressional velocity model was used throughout the core, so the first arriving S-wave beyond about 80 degrees is SKS and beyond about 130 degrees is SKIKS. The small high frequency oscillations (such as between 50 and 90 degrees) in the differential times are the result of the linear interpolation, while the larger offsets are believed to be primarily due to error introduced by the earth flattening transform into the *ttimes* values.

Figure 3. Stylized raypaths for several possible interactions with the 410 km discontinuity to illustrate the use of the TauP phase naming convention. A). Top-side reflections. In all cases, the upgoing phase could be either upper or lower case since the direction is unambiguously defined by the “v” symbol, although lower case is recommended for clarity. B). Transmitted phases. In these cases, there are no alternate forms of the phase names since the symbol case defines the point of conversion from P to S. C). Underside reflections from a surface source. The “^” symbol indicates that the phases reflect off the bottom of the 410. Final wavetype symbol must be upper case, since lower case wavetype symbols are strictly upgoing. D). Interactions for a source depth below the interface. Note that P410s converts on the receiver side just as it does for a surface source in B). However, for a deep source, the phase P410S does not exist since a downgoing P wave cannot generate a downgoing transmitted S wave at an interface below the discontinuity.

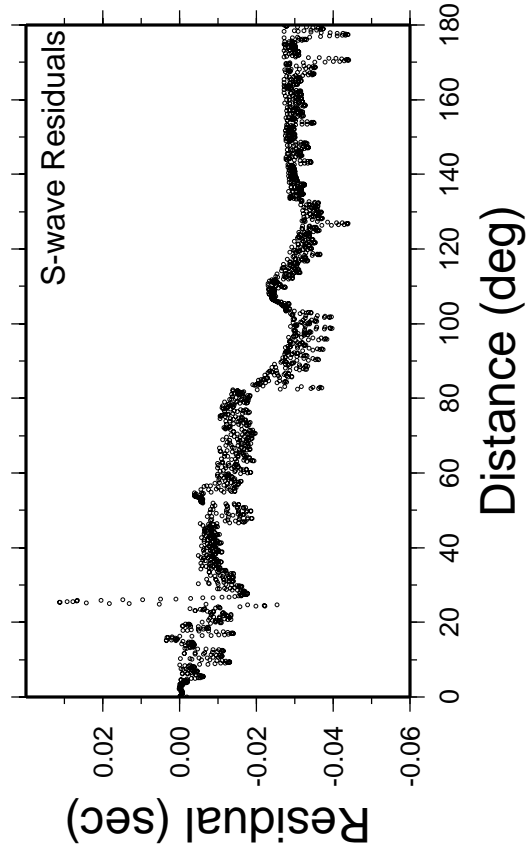
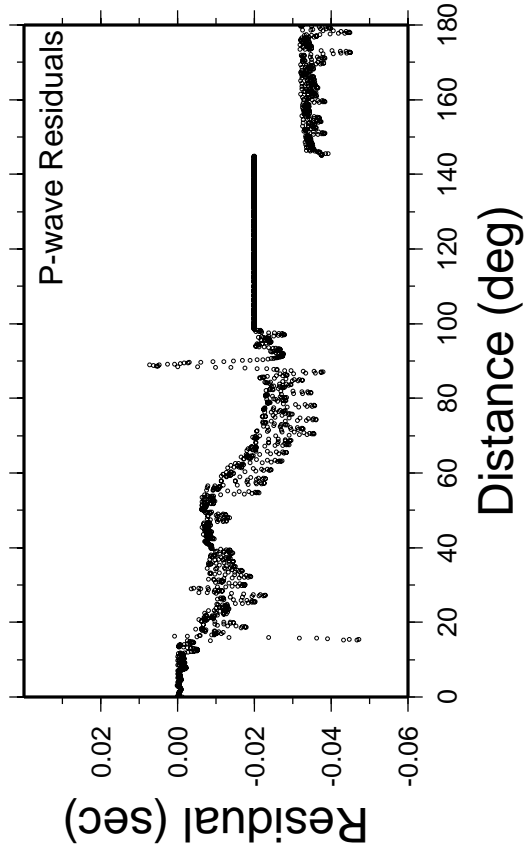
Figure 4. Examples of output from the TauP Toolkit utilities. Some modifications in a touch-up program were done to prepare the figures for publication. A). Output of `taup_path` for the phase $s^{410}PS^{670}PPms$ at a distance of 155 degrees from an event at 630 km depth. $s^{410}PS^{670}PPms$ arrives from both directions, one ray traveling 155 degrees, the other 205 degrees. The model PREM is used. Source is given by the *, station by the triangle. B) Output of `taup_curve` for the same phase as in A). A reducing velocity of 0.125 deg/s was used for this plot. Travel-time curves for PPP, SS, and SKKS are shown for reference. C) Output of `taup_pierce` for the same phase as A) was added to an existing GMT script to produce this output. Points of interaction with the 400 km discontinuity are shown for a hypothetical event near the East Pacific Rise arriving at a hypothetical station in central India. The path for the ray that travels 155 degrees to the station is shown in a solid line and interaction points with the 400 km discontinuity are solid diamonds. The 205 degree raypath is shown as a dashed line with solid circles indicating interaction points at 400 km depth.



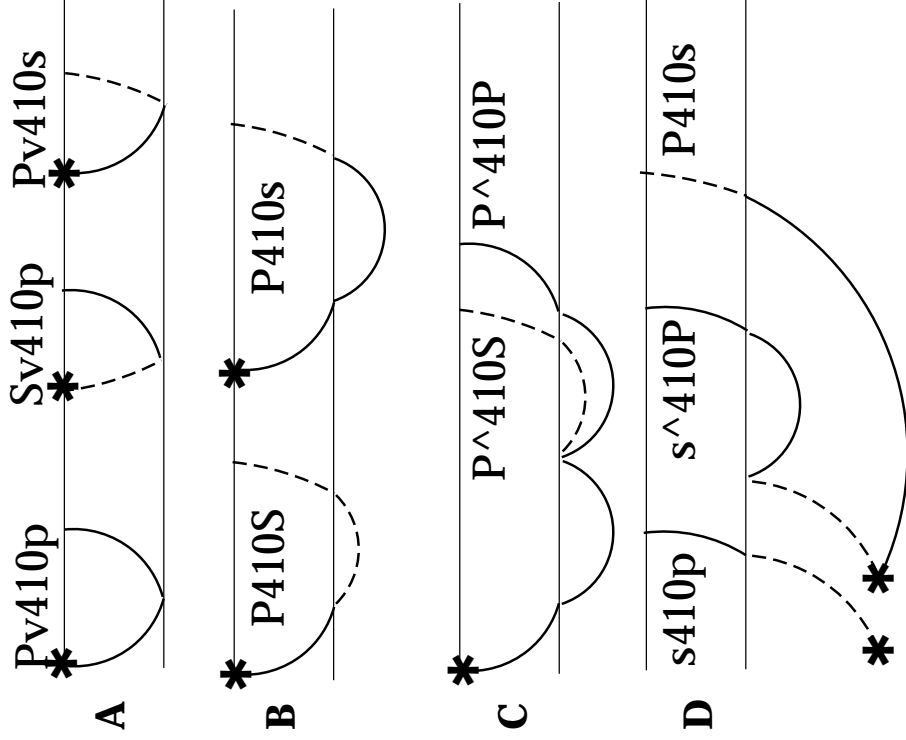
Crotwell et al., Figure 1a



Crotwell et al., Figures 1b



Crotwell et al., Figure 2



Crotwell et al., Figure 3

